Chapter 5

Experimental Results and Discussion

5.1 Introduction

The characterizations of reflective regions and lenticular-lens array will be presented. The aperture size of reflective regions was fabricated in agreement with the designed vales by using proper exposure gap in lithography and sufficient vacuum for sputtering chamber in sputtering. Secondly, self-aligned exposure was utilized to fabricate the lenticular-lens array and several parameters, which influence the shape of lenticular-lens array, were solved and discussed. Finally, the light efficiency and enhancement of lenticular-lens array were measured and then compared with the designed values.

5.2 Reflective Regions

According to the simulation results presented in chapter 4, the aperture size of reflective region (AP) can influence the light efficiency and enhancement. Larger aperture size of reflective regions decreases the light efficiency in reflective mode. In contrast, smaller aperture size of reflective region reduces the light efficiency in transmissive mode. Besides, in self-aligned exposure process, defocus effect was utilized to fabricate lenticular-lens array, thus, the aperture size of reflective regions was expected to be one of key parameters to determine the characteristics of lenticular-lens structure, as illustrated in Fig. 5.1. As a result, AP must be fabricated as accurate as possible.

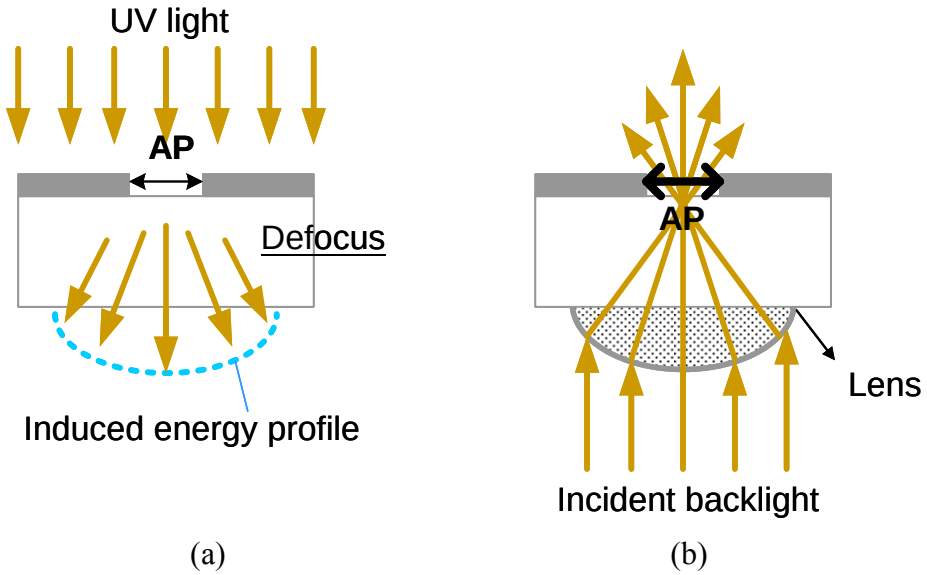

Fig. 5.1. Illustrations of the influence of aperture size of reflective region (AP) on (a) fabrication of lenticular-lens structure and (b) application of improving light efficiency

From the previous experimental results, larger exposure gap in lithography process would cause a ladder-shaped photoresist pattern and then, in sputter process, metal film would cover the surface of photoresist completely, thus, the reflective regions could not be obtained by using lift-off, as depicted in Fig. 5.2.

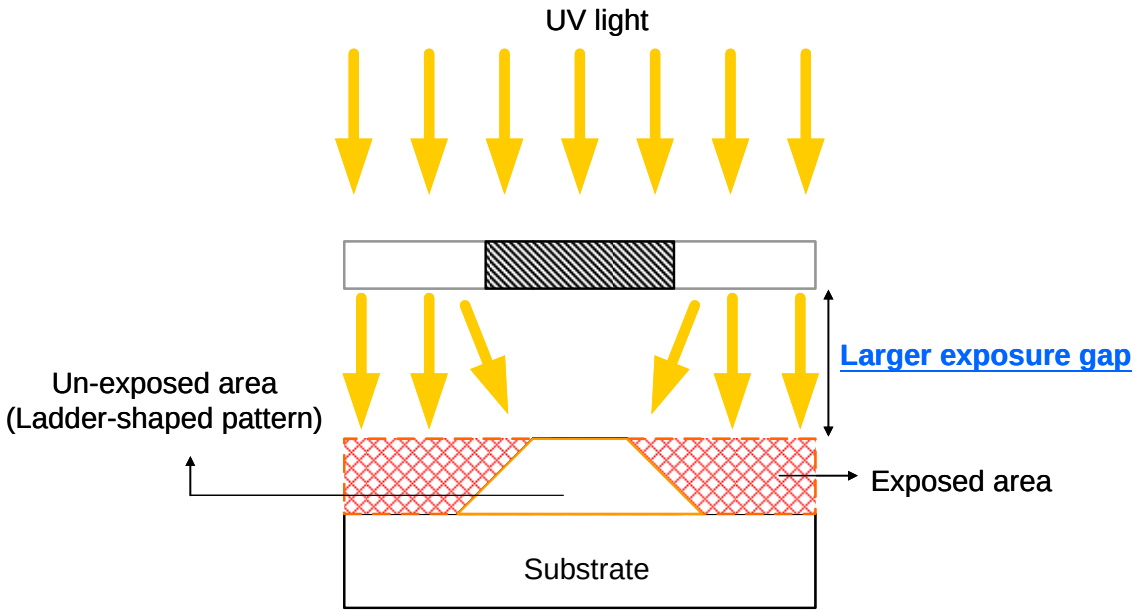

Fig. 5.2. Illustration of ladder –shaped photoresist patterns caused by larger exposure gap

Hypothesize mentioned above could be examined by measured results, as shown in Fig. 5.3. In this case, the width of shadow area on mask was designed to be 28um. In other words, the width of exposed photoresist would be 28um. However, due to larger exposure gap, ladder-shaped patterns were formed. The measured widths of top and bottom surfaces were 25.7um and 36um, respectively. In addition, the thickness of ladder-shaped pattern was 5.2um. Consequently, in sputter process, metal film would cover the structure completely and resulted in the failure of lift-off. In order to overcome this issue, the exposure gap was reduced in the following fabrication.

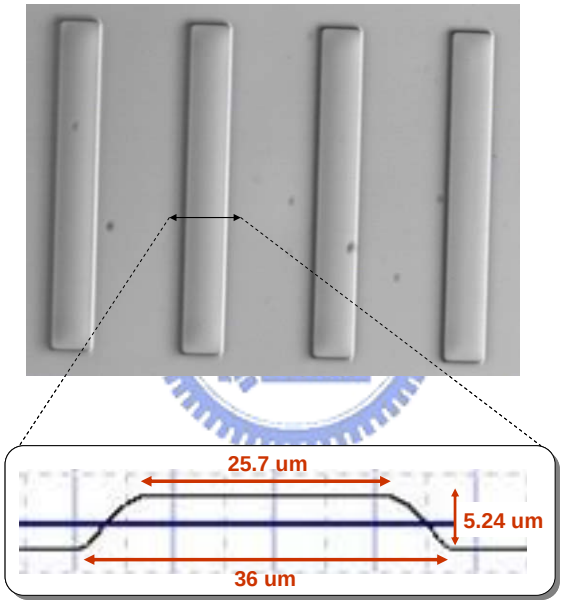

Fig. 5.3. Measured result of ladder –shaped photoresist patterns covered by metal film

Besides the issue of exposure gap, vacuum of sputter chamber also influenced the uniformity of metal film covering the patterned photoresist, as depicted in Fig. 5.4. Insufficient vacuum (pressure of chamber > $5*10^{-6}$ torr) results in rough metal film covering the patterned photoresist, thus, causing non-uniform reflective regions on whole patterned area. In order to overcome the problem, vacuum of sputter chamber shall be low enough.

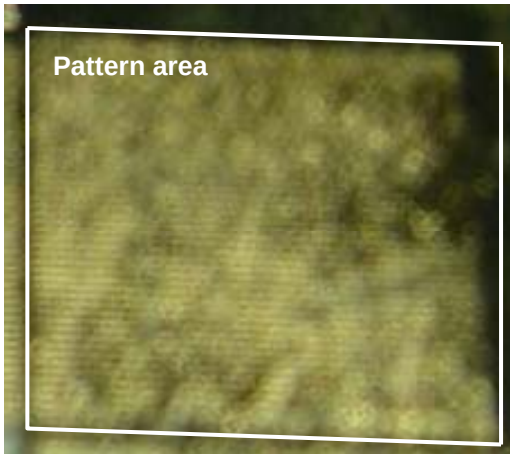

Fig. 5.4. Illustrated figure of non-uniform metal film after sputter process

It is worth noting that AP not only influences the light efficiency but also affects the features of lenticular-lens array. Therefore, the reflective regions with various aperture sizes were fabricated. Based on implementing the proposed solutions described above, the relationship of designed and fabricated aperture size of reflective regions could be obtained, as shown in Fig. 5.5. It is obvious that the error of aperture size between fabricated and designed structures is of less than 5% to -5%. We can, therefore, reasonably conclude that the fabrication conditions used to form reflective regions with acceptable aperture size were obtained.

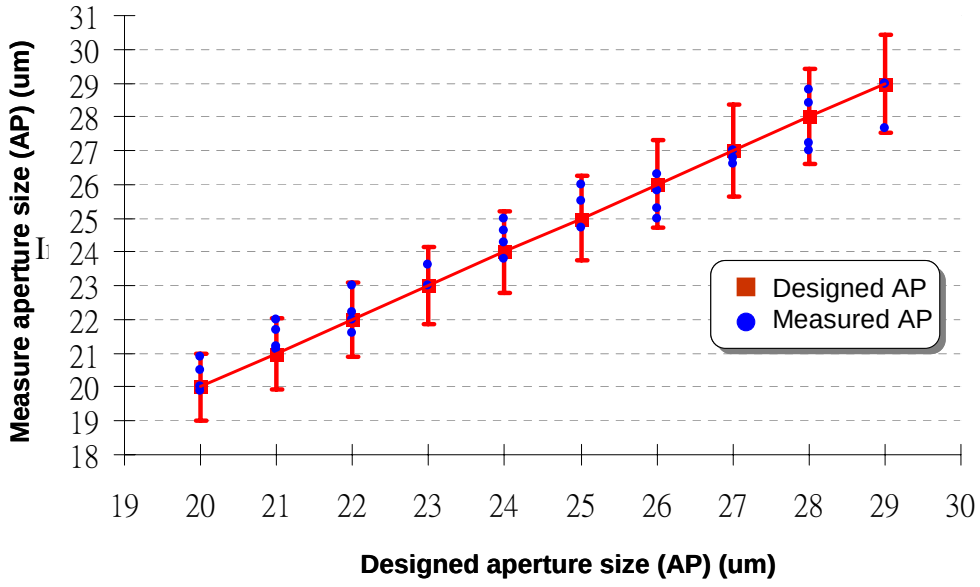

Fig. 5.5. Interpretation of the relationship between designed and fabricated aperture size of reflective regions

5.3 Lenticular-lens Array

After forming reflective regions with various aperture sizes, Lenticular-lens array, which is composed of a transparent photoresist, was implementing by self-aligned exposure and then the characteristics of lenticular-lens array was measured by surface profile and SEM in the following sections. Besides, some issues occurred in the fabrications process was described and solved.

5.3.1 Diffraction Effect

According to the conventional lithography conditions, an undesirable structure was formed as the exposure time ranging from 3second to 9second, as depicted in Fig. 5.6. In general, the shape of exposed photoresist was related to the energy profile of UV light illuminating on photoresist so that, in this case, a two-peak-like energy profile was expected to be induced by diffraction effect and then resulted in the undesirable structure.

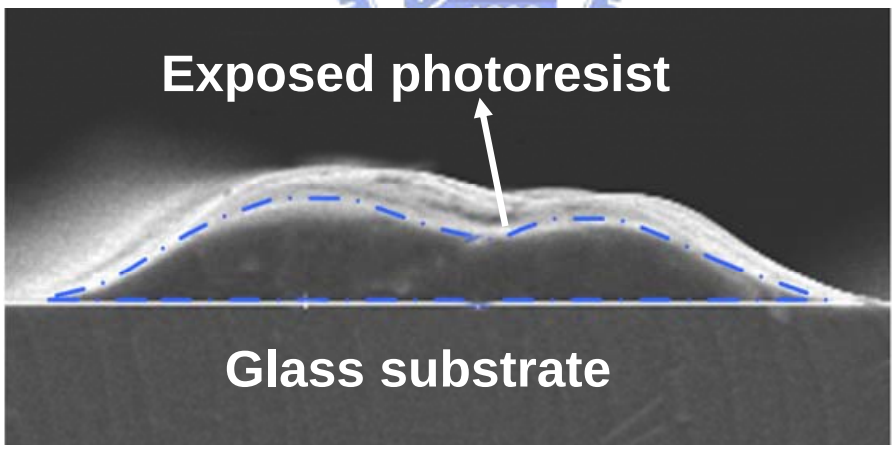

Fig. 5.6. SEM diagram of exposed structure as the exposure time varied from 3second to 9second

Based on diffraction theory [18], the Fresnel number, which can justify the type of diffraction, was derived as Equation (5).

$$N_f = \frac{(AP)^2}{\lambda d} \quad \text{.....(5)}$$

, where N_f is the

Fresnel number, AP is the aperture size of reflective regions, λ is the wavelength of UV light and d is the propagation distance. Fig. 5.7 helps to clearly define the meaning of each parameter. Take the optimized specifications as example, when AP equaled 22um, d equaled 700um and λ equaled 0.365um, N_f was 1.89, thus, Fresnel diffraction was resulted. As a result, the energy profile was not a peak-like shape and then the lenticular-lens structure could not be obtained.

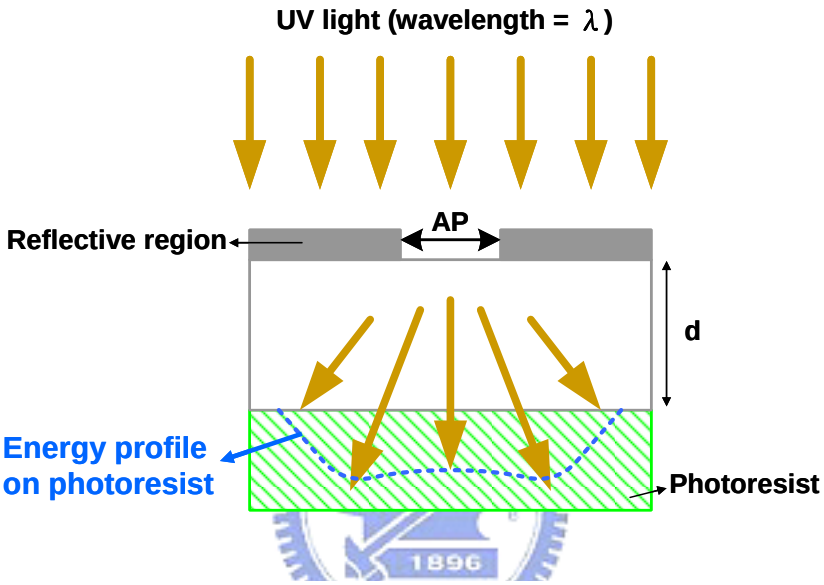

Fig. 5.7. Schematic diagram of definitions of aperture size of reflective region (AP), propagation distance (d) and wavelength of UV light (λ)

5.3.2 Shape of Exposed Photoresist

In order to compensate the diffraction effect, the exposure time was increased from 10second to 50second at 10second intervals to restructure the shape of exposed photoresist. Some sampled fabricated results were shown in Fig. 5.8. The structures illustrated in Figs. 5.8 (a), (b) and (c) were fabricated with the exposure time of 20second, 30second and 50second, respectively. It is apparent that the shape of exposed photoresist changed as the exposure time varied from 20second to 50second. Besides, the thickness of exposed structure was increased from 8.3um to 10.4um, respectively, as the exposure time raising. The reason could be described as follows.

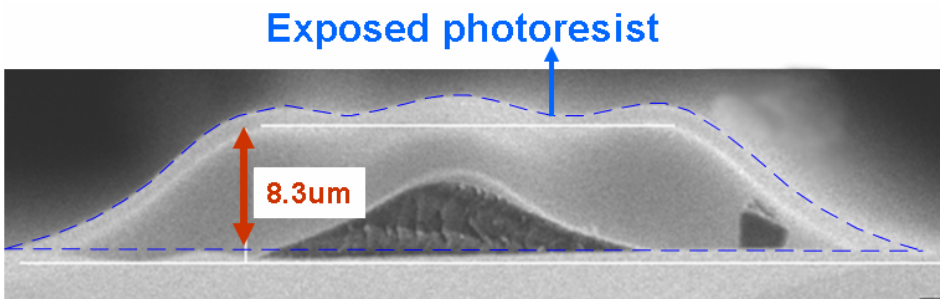

(a)

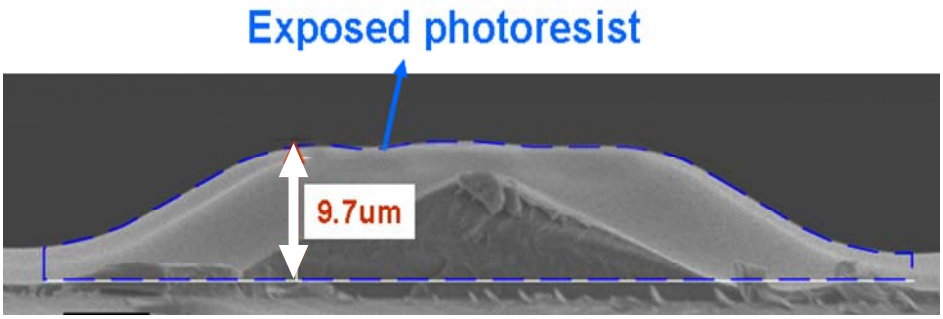

(b)

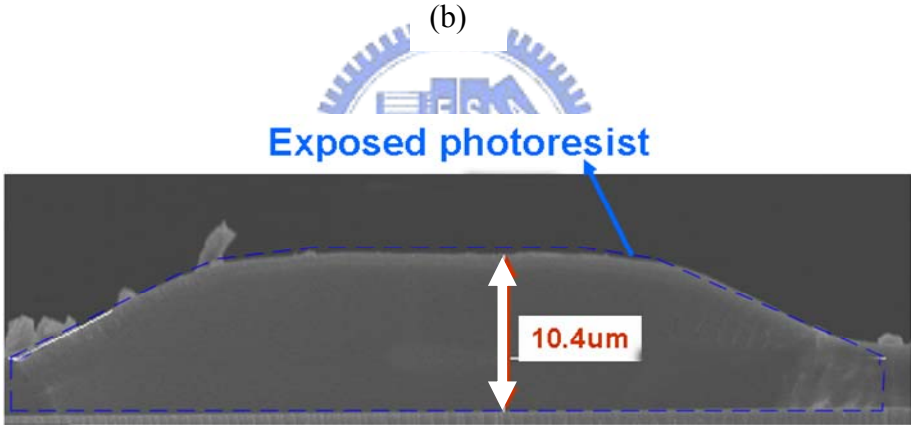

(c)

Fig. 5.8. SEM diagrams of exposed photoresist with the exposure time of (a) 20second, (b) 30second and (c) 50second, respectively

As the exposure time increased, the energy absorbed by photoresist would be accumulated and then the shape of exposed photoresist could be restructured. In this case, the thickness of photoresist before exposed by UV light was about 11um. When exposure time was 20second, the energy profile could be illustrated as the dash line in Fig. 5.9 (a). The area with oblique stroke was defined as the exposed photoresist. The

energy on A region was larger than that on B region, thus, the shape of exposed photoresist was a wave-like profile. In additional, the thickness of exposed photoresist was 8.3um, which was of less than 11um. When exposure time was increased to 30second, the photoresist absorbed much energy and resulted in thicker thickness of exposed structure, as depicted in Fig. 5.9 (b). Besides, the profile of exposed photoresist was more flat compared to Fig. 5.9 (b). This phenomenon can be explained by the characteristic of photoresist. Photoresist must absorb a critical energy and then the exposed area will be cross-linked. As shown in Fig. 5.9 (b), C regions were illuminated by UV light but the absorbed energy was not larger than the critical energy, thus, the photoresist on C regions could not be cross-link. Consequently, the wave-like profile was not so apparent. When exposure time was increased to 50second, the thickness of exposed structure was 10.4um, which was almost equal to the thickness of photoresist before exposed. This phenomenon depicted that all the photoresist on D region was almost exposed, thus, the surface profile on D region was very flat, as illustrated in Fig. 5.9 (c). From the above explanations, a structure with circular surface could not be obtained as the exposure time was 20second to 30second. In contrast, during 30second to 50second, the top surface of exposed structure was flatter and resulted in a flat-top lens structure.

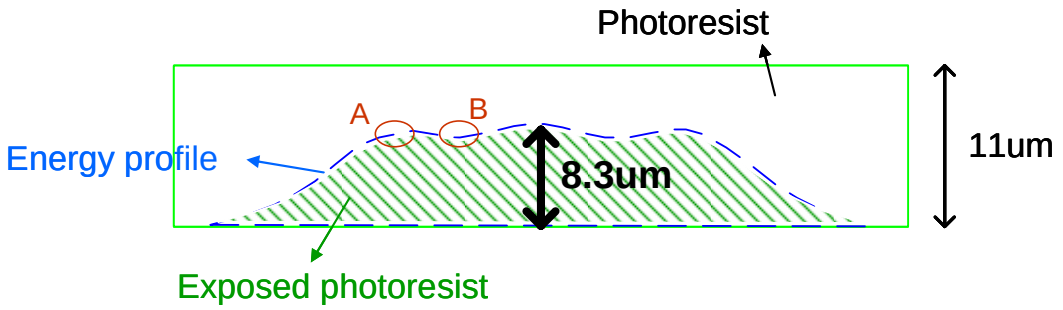

(a)

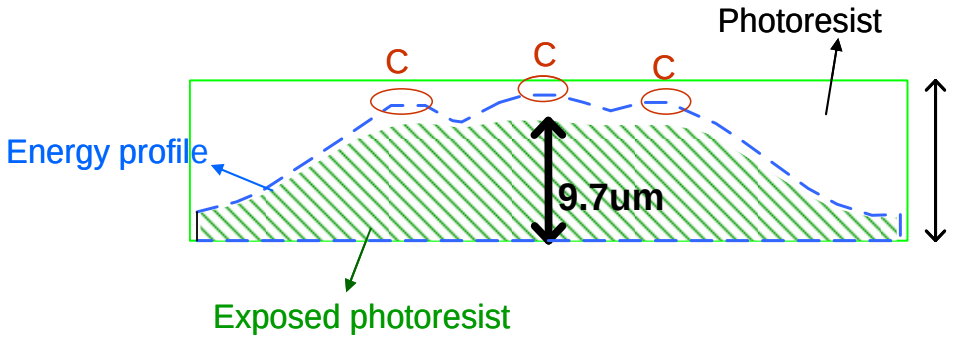

(b)

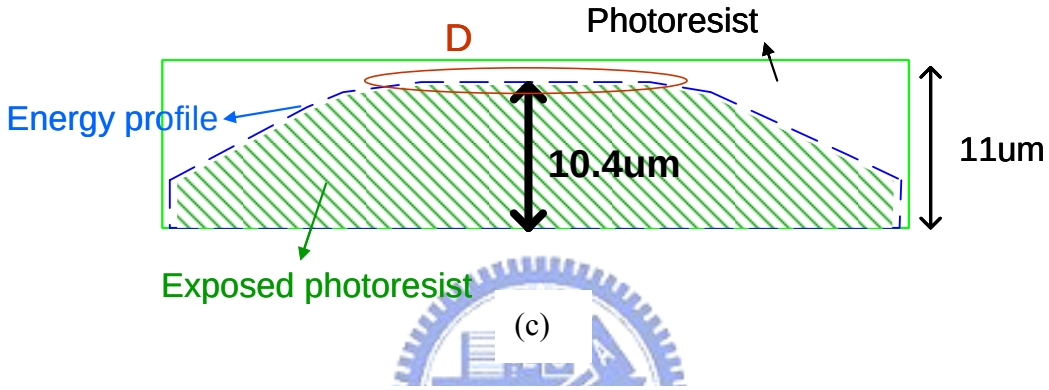

(c)

Fig. 5.9. Illustrations of exposed structure with the exposure time of (a) 20second, (b) 30second and (c) 50second, respectively

Although a flat-top lens structure could be obtained during 30second to 50second, this profile was not good enough, thus, the exposure time varied from 10second to 20second at 1second intervals was demonstrated. One of the fabricated results was shown in Fig. 5.10. It is obvious that a lensticular-lens structure could be obtained. From the fabrication results, as the exposure time ranging from 3second to 50second, exposed structures with various surface profiles could be formed. During 10second to 20second, aspheric lensticular-lens structure would be obtained. However, for the optimized structure, the surface of the lensticular-lens structure was spherical. Therefore, the method, which utilized a UV light with divergent angle, was proposed to solve this issue in the following experiments.

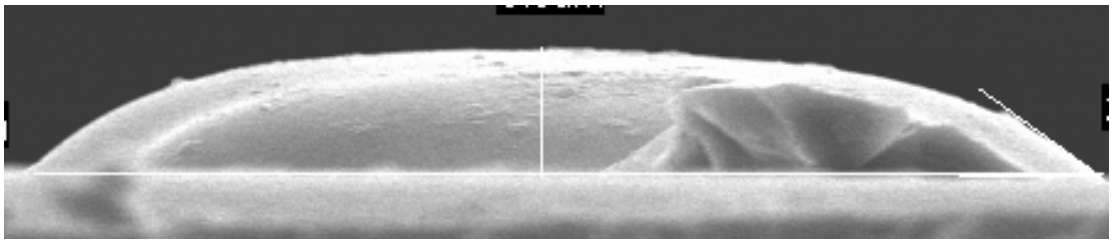

Fig. 5.10. SEM diagram of a lensticular-lens structure with aspheric surface profile

5.4 UV Light with Divergent Angle

According to diffraction theory, for periodic silts with fixed aperture size, a diffraction effect is easier to yield as a collimated light source passing through the periodic silts. In contrast, the diffraction effect is not remarkable when utilizing a light source with divergent angle. Therefore, a UV light with divergent angle was utilized to avoid diffraction effect and then a lenticular-lens structure with spherical surface could be obtained.

5.4.1 Excimer Laser

Based on the configuration of excimer laser system, the UV light for exposing photoresist is formed by a condensing lens system. Thus, properly adjusting the condensing lens system, a UV light with divergent angle can be obtained. As a result, excimer laser system was utilized as a light source for self-aligned exposure. Fig. 5.11 illustrated the fabrication of lens structures formed by excimer laser system. It is apparent that a peak-like structure could be obtained. However, the size of lens array on the marginal part of exposed area was smaller than that on the central part of exposed area. The reason is that the divergent angle of UV light was too large, thus, causing non-uniform energy distribution and then the size of lenticular-lens array on central and marginal parts were not the same. Besides, the surface of the fabricated

lenticular-lens array was not smooth enough. As a result, a UV light with smaller divergent angle, which is less than that of excimer laser system, was proposed to fabricate the lenticular-lens structure in the following sections.

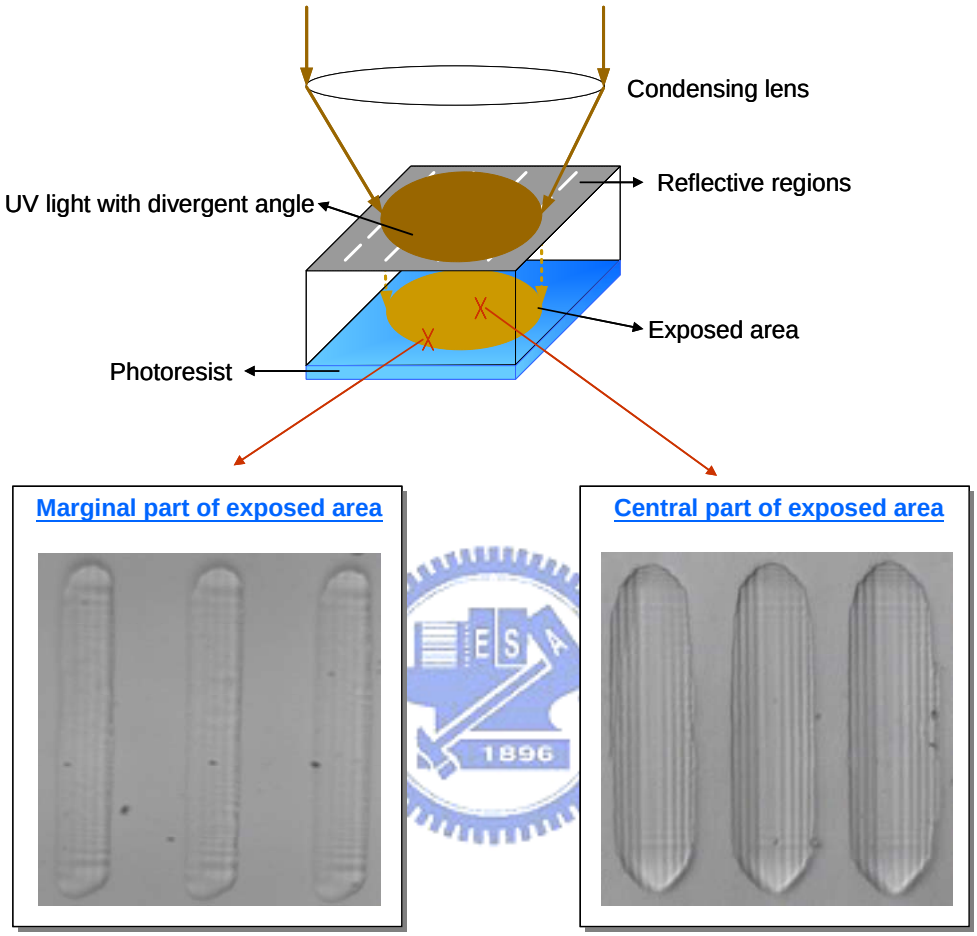

Fig. 5.11. Graphical diagram of the lenticular-lens array fabricated by excimer laser system

5.4.2 UV Light with Smaller Divergent Angle

The UV light with smaller divergent angle was utilized to fabricate the lenticular-lens structure. Because the divergent angle was not as large as that of excimer laser, thus, the energy distribution was more uniform both on marginal and central parts of exposed area.

5.4.2.1 Characteristics of Lenticular-lens Structure

According to the simulated results shown in chapter 4, the lenticular-lens structure with specifications, of which radius (R) and diameter (D) of lenticular-lens structure and aperture size (AP) of reflective regions are 66um, 68um and 22um, respectively, was chosen for applications. However, in fabrications, AP would influence the radius and diameter of lenticular-lens structure and then resulted in changing the spot size of collected backlight to decrease the light efficiency in transmissive mode. Therefore, in the following experiments, the objective was to achieve a lenticular-lens structure with R=66um and D= 68um, and AP could be changed. Besides, due to the limitations of measurements, the radius of lenticular-lens structure was not ease to measure, thus, the thickness and diameter of lenticular-lens structure were measured to derive the radius of lenticular-lens structure. The relationship between radius, diameter and thickness of lenticular-lens structure was derived as Equation (6).

$$R = \frac{T^2 + D^2/4}{2*T} \quad \text{.....(6)}$$

, where T is the thickness of lenticular-lens structure. Based on Equation (6), when T=9.4um and D = 68um, a lenticular-lens structure with R=66um could be obtained. As a result, a lenticular-lens structure with T=9.4um and D=68um was fabricated to obtain a radius of 66um. Because the aperture size of reflective regions and exposure time would determine the features of lenticular-lens structure, the relationships between these parameters were analyzed as follows.

When the thickness of photoresist without exposing was around 14um and the exposure time was fixed, the relationship between thickness of lensticular-lens structure and aperture size of reflective regions was illustrated in Fig. 5.12. As AP varied from 20um to 29um, T would range from 12.5um to 14um. Although the

tendency of T did not behave regularly but its variation could be within 1.5um, indicating a minor impact of AP on T. Therefore, in the following experiments, the thickness of lensticular-lens structure was controlled to be around 9um by tuning the exposure time.

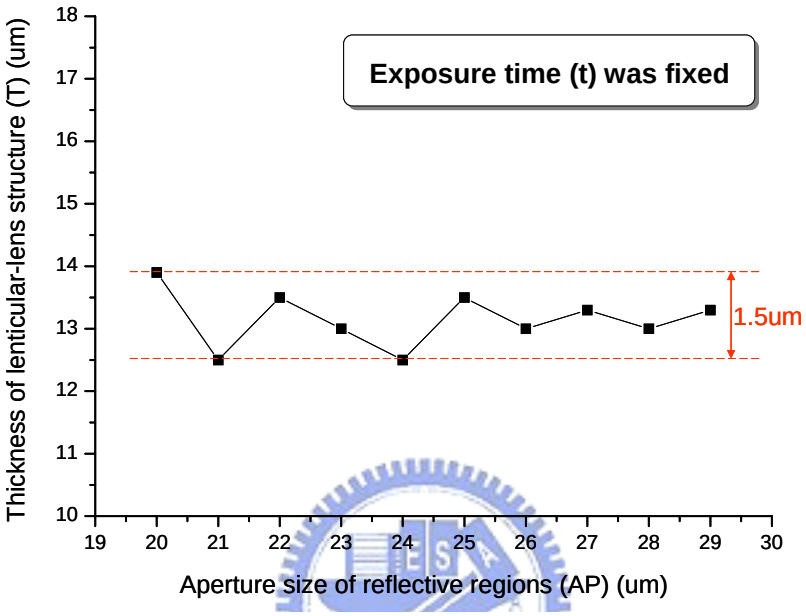

Fig. 5.12. Interpretation of the relationship between the aperture size of reflective regions and the thickness of lensticular-lens structure

In order to clearly illustrate the relationship between exposure time and thickness of lensticular-lens structure, the aperture size of reflective regions was chosen as 25um, here. The SEM diagrams of fabricated structures with the exposure time of 5 second, 10second and 15second are shown in Figs. 5.13 (a), (b) and (c), respectively. T_B was defined as the size of the base of lensticular-lens structure causing by interference. Obviously, as exposure time changed from 5second to 15second, T decreased from 13.5um to 10.5um and T_B increased to 3um, respectively. The tendencies of T and T_B were proportional and inversely proportional to exposure time, respectively. However, as exposure time raised from 5second to 15second, D would achieve a minimum value of 62um at t=10second. This effect was caused by the interference of two adjacent energy profiles. The detail illustrations were shown in Fig.

5.14. The solid line represented the energy profile absorbed by photoresist and the area with oblique stroke was illustrated as the lenticular-lens structure. The thickness of photoresist before exposing was around 13.5um.

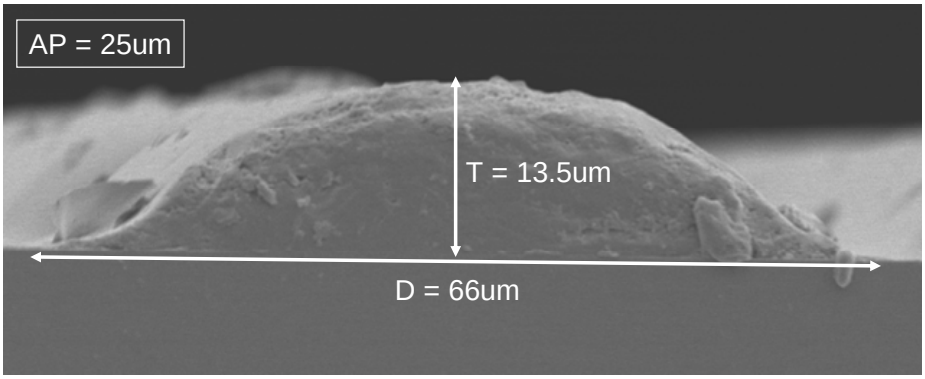

(a)

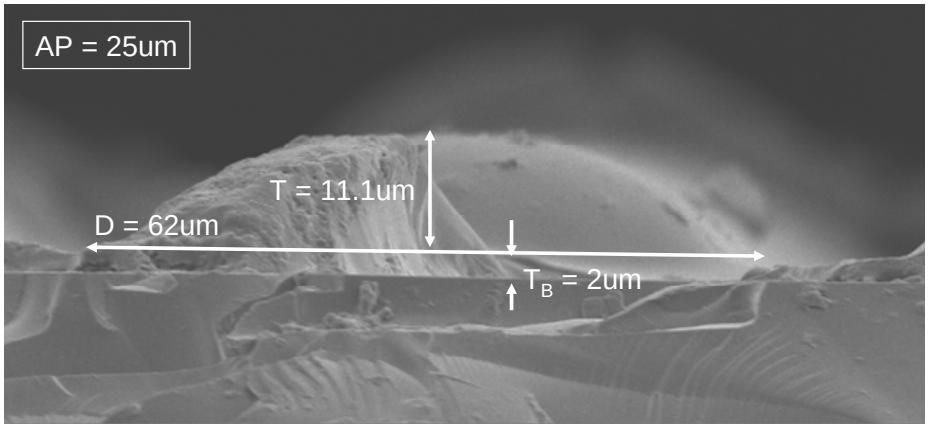

(b)

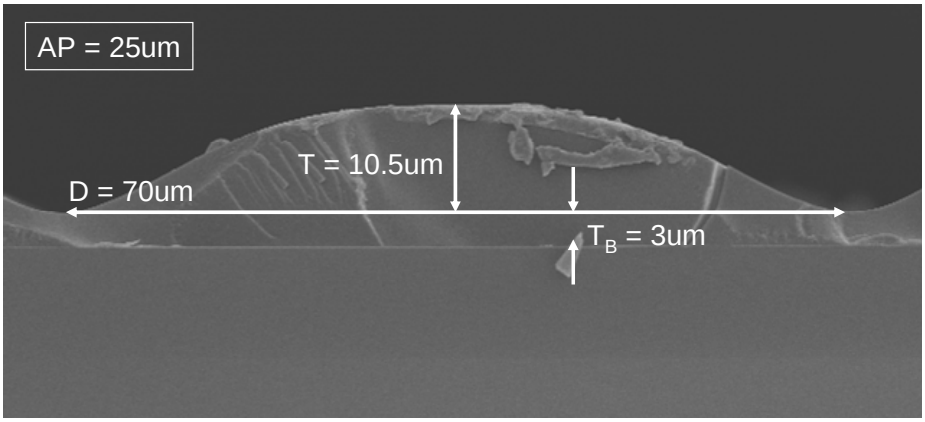

(c)

Fig. 5.13. Illustration of the features of lenticular-lens structures with exposure time of (a) 5second, (b) 10second and (c) 15second, respectively

When exposure time was 5second, the energy profiles between two adjacent areas did not interfere each other, as depicted in Fig. 5.14 (a), i.e. the diameter of lenticular-lens structure did not achieve 70um. However, as exposure time increased to 10second, the energy profile was extended simultaneously, Consequently, interference effect would apparent between two adjacent areas and then resulted in producing the base of lenticular-lens structure, thus, the thickness and diameter of lenticular-lens structure was reduced to 11.1um and 62um, respectively, as shown in Fig. 5.14 (b). In this case, T_B was 2um. The thickness of lenticular-lens structure added TB approached the thickness of photoresist before exposing. In the following, exposure time was increased to 12second, for example, and then T_B was raised to 3um. Besides, T and D were decreased to 10.5um and 60um, respectively, as illustrated in Fig. 5.14 (c). Finally, when exposure time increased to 15second, the energy profiles was extended continuously, as a result, D could increase to 70um, as described in Fig. 5.14 (d). If exposure time was kept on increasing, TB would be larger than 3um and T and D would reduce again.

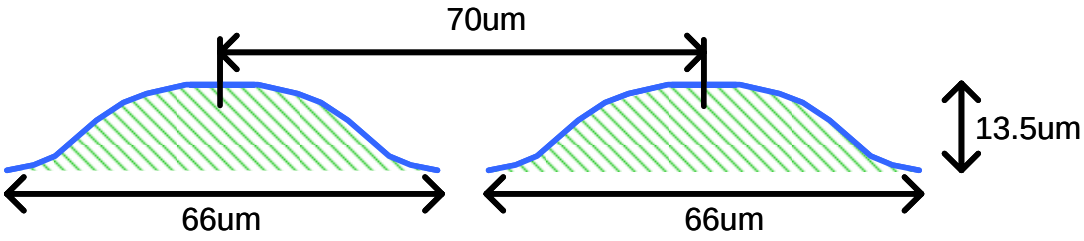

(a)

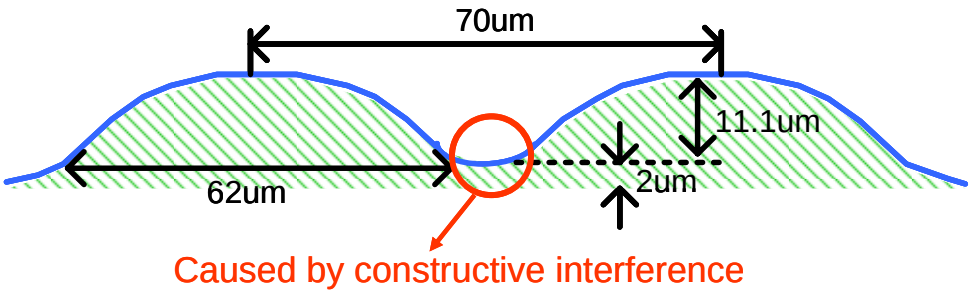

(b)

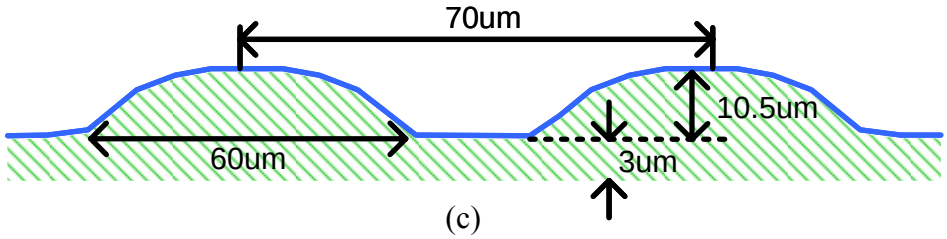

(c)

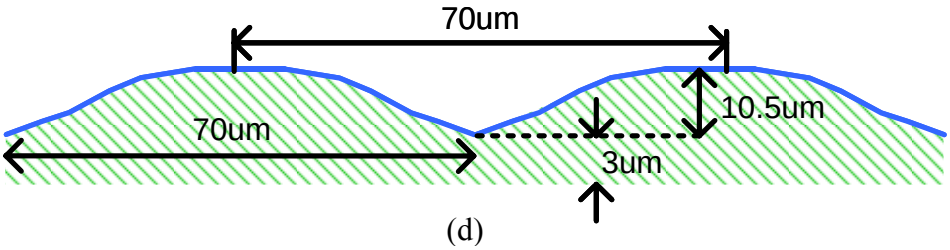

(d)

Fig. 5.14. Illustrations of interference effect with exposure time of (a) 5second, (b) 10second, (c) 12second and (d) 15second, respectively

Because 15second of exposure time could produce a lenticular-lens structure with a 10.5um of thickness, which is relatively close to the target of 9.4um thick, therefore, exposure time was fixed as 15second and the relationships between the aperture size of reflective regions, diameter and thickness of lenticular-lens structure were demonstrated, as shown in Fig. 5.15. D curve represented the relationship between AP and D, and T curve represented the relationship between AP and T. Obviously, as AP changed from 20um to 29um, D and C curves performed like waves. This phenomenon also caused by interference effect. Although exposure time was fixed, but different AP would produce different energy profile, thus, interference effect was apparent as AP varied within some range. As a result, the tendencies of T and D were presented as shown in Fig. 5.15. In this case, T was changed within the range from 10um to 8um and D changed from 65um to 70um as AP varied from 25um to 29um, therefore, exposure time was slightly adjusted to find the optimized lenticular-lens structure with T=9.4um and D=68um. Finally, the lenticular-lens structure with specifications of R=66um, D=68um and AP=27um was demonstrated. The top-view of fabricated structure is shown in Fig. 5.16.

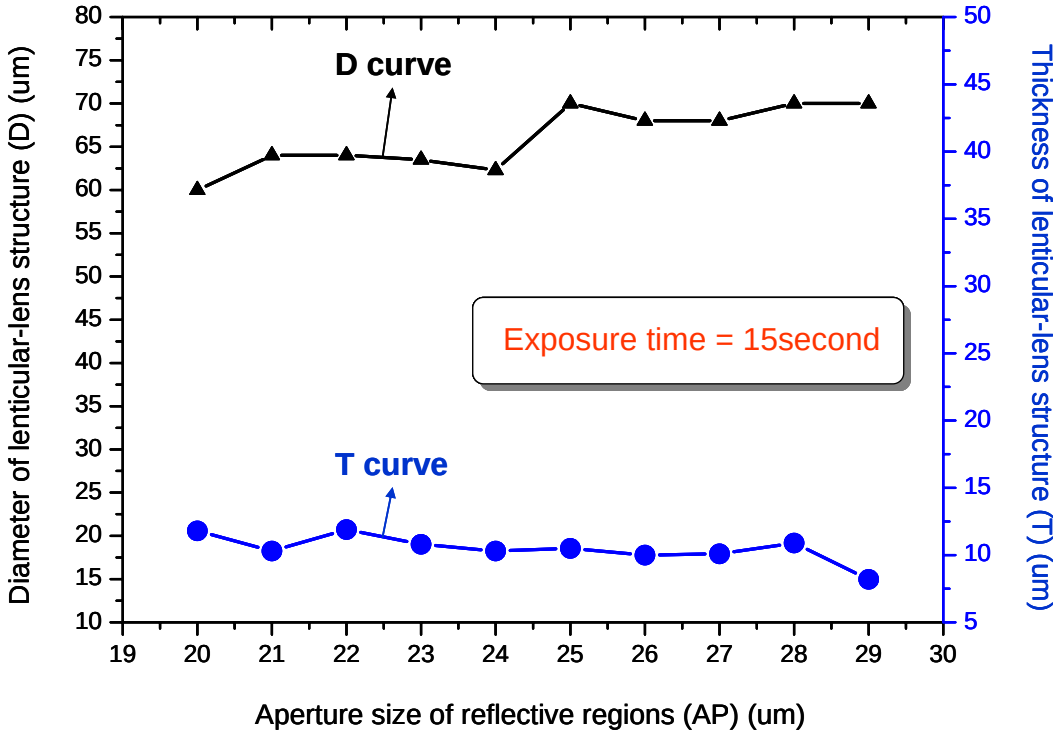

Fig. 5.15. Illustrations of the tendencies of thickness (T) and (D) of lenticular-lens structure as the aperture size of reflective regions (AP) changed from 20um to 29um

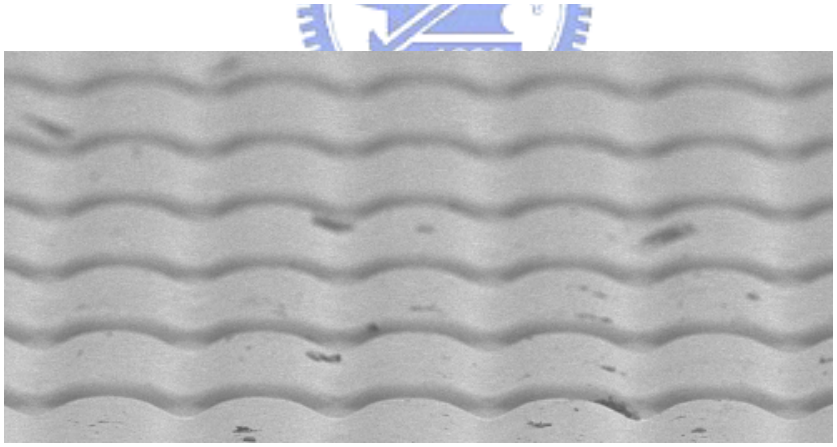

Fig. 5.16. SEM diagram of lenticular-lens array with radius of 66um and diameter of 68um as the aperture size of reflective regions equals to 27um

5.4.2.2 Light Efficiency and Efficiency Enhancement

After the whole fabrication, an optical measurement system-ELDIM was utilized to measure the transmissive light utilization efficiency of lenticular-lens array structure for proposed directional backlight and a commercial collimated backlight,

ORMON backlight [19]. The measured light efficiency was defined as the ratio of the integrated intensity of the measured sample plus backlight to that of backlight. For example, the light efficiency of conventional structure was the ratio of the integrated intensity of conventional structure plus backlight to that of backlight. The unit of integrated intensity is lm/m^2. Besides, the light efficiency enhancement was defined as the ratio of light efficiency of lenticular-lens array to conventional structure.

5.4.2.2.1 Directional Backlight

The angular distribution of proposed directional backlight was shown in Fig. 5.17. The divergent angle along horizontal and vertical directions were 15° and 60°, respectively. According to the measured results, the light efficiency enhancement produced by lenticular-lens array was not noticeable when using directional backlight as light source. The reason is described as follows. In simulation, the divergent angle in horizontal and vertical directions are both within 15°. However, from measured results, the divergent angle along vertical direction is 40°, thus, the energy distribution of fabricated directional backlight is not similar to that of designed backlight, thus, resulting in unapparent light efficiency enhancement.

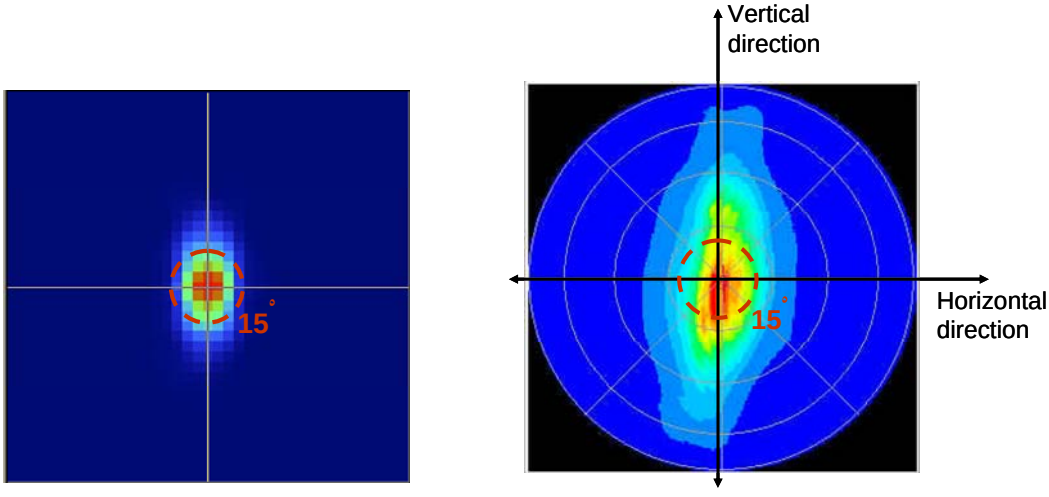

(a) (b)

Fig. 5.17. Angular distributions of (a) the designed directional backlight and (b) the fabricated directional backlight

5.4.2.2.2 OMRON Backlight

The angular distribution of OMRON backlight was shown in Fig. 5.18. The divergent angle along horizontal and vertical directions were both within 15°, which were similar to the simulation results, therefore, OMRON backlight was utilized to evaluate the performance of lenticular-lens array. The light efficiency of conventional structure with AP=35um was 0.5. The light efficiency of fabricated lenticular-lens array with specifications of R=66um, D=68um was 0.7. From calculation, 1.4 of gain factor could be obtained. It is evident that lenticular-lens array can collect the incident backlight and then enhance the transmissive light efficiency. The luminance plot of proposed and conventional structures is show in Fig. 5.19. The dash line and solid line are represented the luminance plots of conventional and proposed structures, respectively. It presents that the lenticular-lens array can result in a broadening of the distribution to a width of ±30°. Moreover, it is apparent that the intensity around 0° dose not increase, but the light that without lenses would arrive at locations outside the aperture of reflective regions, then, is redistributed to come inside the aperture of reflective regions at larger angles. Although the measured gain factor was not as high as the designed gain factor, the reasons can be explained as follows. The simulation software, ZEMAX, only can provide a divergent point source, but OMRON backlight is a surface light source, thus, the real spot size will be larger than the designed value and then influences the light efficiency. In addition, the reflection at the interface between two different media also decreases the light utilization. In general applications, anti-reflection film will be formed on the surface of lens, thus, resulting in decreased the loss caused by reflection. However, in our experiments, lenticular-lens structure was not coated with an anti-reflection film and then partial energy would be lost. Finally, the fill factor of fabricated structure is not as high as the designed structure, as shown in Fig. 5.20. Therefore, the amount of collected

backlight is not equal to the expected value and then resulting in the influence of light efficiency enhancement.

Among the three reasons mentioned above, increasing fill factor of lenticular-lens array is a more feasible method, thus, a compensated reflective regions were used, as shown in Fig. 5.21. By using the compensated reflective regions, a lenticular-lens array could be fabricated. The top-view of the fabricated lenticular-lens array was shown in Fig. 5.22. From calculation, the fill factor was increased to 0.92 by adopting the compensated reflective regions.

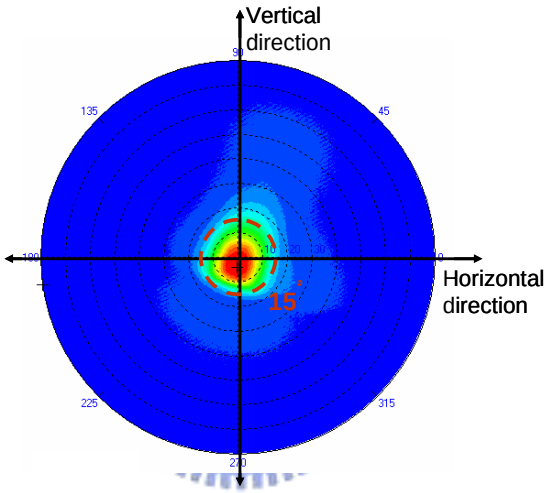

Fig. 5.18. Angular distributions of OMRON backlight

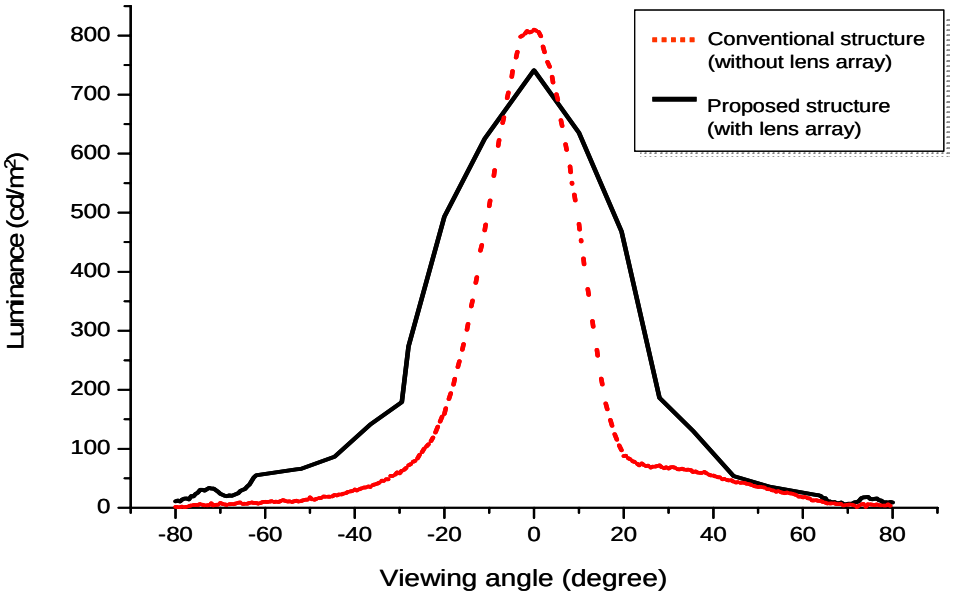

Fig. 5.19. Luminance plots of conventional and proposed structures

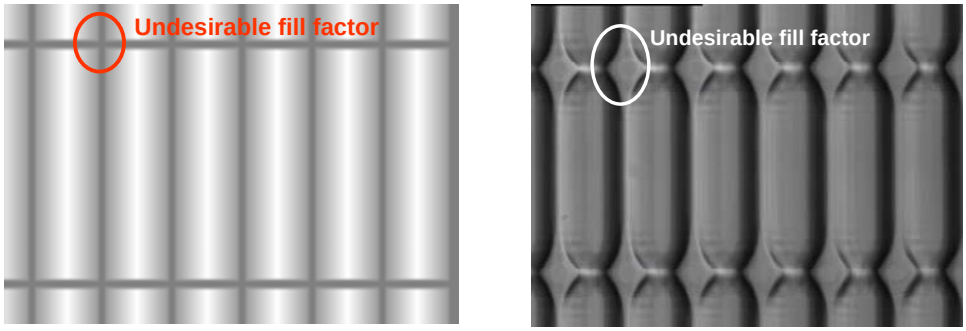

(a) (b)

Fig. 5.20. Illustrations of fill factor of (a) designed and (b) fabricated structure

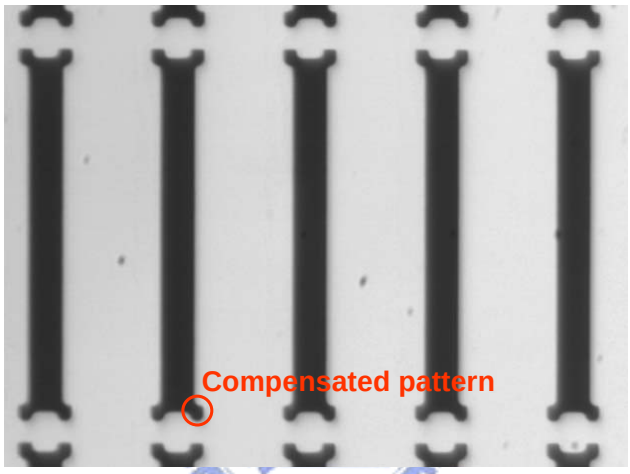

Fig. 5.21. Illustration of reflective regions with compensated patterns

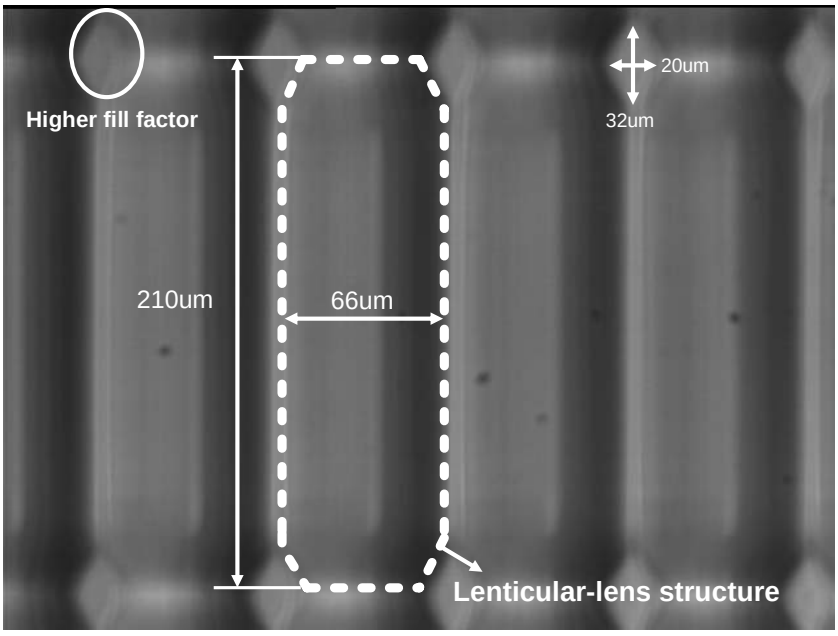

Fig. 5.22. Photograph of lenticular-lens array with higher fill factor

5.5 Summary

By using self-aligned exposure which utilized a UV light source with small divergent angle, a lenticular-lens array structure with R=66um, D=68um and AP=27um was fabricated. In addition, 1.4 of gain factor in transmissive mode could be obtained when using OMRON backlight as light source. It can be concluded that the lenticular-lens array can collect backlight and enhance the backlight efficiency. Although the gain factor is not as high as the designed value, it can be further enhanced by reducing the loss in reflection and increasing the fill factor of lenticular-lens array. Finally, a lenticular-lens array with higher fill factor was demonstrated by using the compensated reflective regions.